



# GENOME RESEARCH

## Contiguous and complete assemblies of *Blastocystis* gut microbiome-associated protists reveal evolutionary diversification to host ecology

Abigail L. Lind, Nathan A. McDonald, Elias R. Gerrick, et al.

*Genome Res.* 2025 35: 1377-1390 originally published online April 22, 2025  
Access the most recent version at doi:[10.1101/gr.279080.124](https://doi.org/10.1101/gr.279080.124)

---

**References** This article cites 86 articles, 9 of which can be accessed free at:  
<http://genome.cshlp.org/content/35/6/1377.full.html#ref-list-1>

**Open Access** Freely available online through the *Genome Research* Open Access option.

**Creative Commons License** This article, published in *Genome Research*, is available under a Creative Commons License (Attribution-NonCommercial 4.0 International), as described at <http://creativecommons.org/licenses/by-nc/4.0/>.

**Email Alerting Service** Receive free email alerts when new articles cite this article - sign up in the box at the top right corner of the article or [click here](#).



To subscribe to *Genome Research* go to:  
<https://genome.cshlp.org/subscriptions>

---

## Research

# Contiguous and complete assemblies of *Blastocystis* gut microbiome-associated protists reveal evolutionary diversification to host ecology

Abigail L. Lind,<sup>1,2</sup> Nathan A. McDonald,<sup>2,3</sup> Elias R. Gerrick,<sup>4</sup> Ami S. Bhatt,<sup>5,6</sup> and Katherine S. Pollard<sup>1,7,8</sup>

<sup>1</sup>Gladstone Institute for Data Science and Biotechnology, Gladstone Institutes, San Francisco, California 94158, USA; <sup>2</sup>School of Biological Sciences, Georgia Institute of Technology, Atlanta, Georgia 30332, USA; <sup>3</sup>Department of Biology, Stanford University, Stanford, California 94305, USA; <sup>4</sup>Department of Microbiology, University of Chicago, Chicago, Illinois 60637, USA; <sup>5</sup>Department of Genetics, Stanford University, Stanford, California 94305, USA; <sup>6</sup>Department of Medicine (Hematology, Blood and Marrow Transplantation), Stanford University, Stanford, California 94304, USA; <sup>7</sup>Department of Epidemiology and Biostatistics, University of California, San Francisco, California 94158, USA; <sup>8</sup>Chan Zuckerberg Biohub SF, San Francisco, California 94158, USA

*Blastocystis*, an obligate host-associated protist, is the most common microbial eukaryote in the human gut, and is widely distributed across vertebrate hosts. The evolutionary transition of *Blastocystis* from its free-living stramenopile ancestors to a radiation of host-associated organisms is poorly understood. To explore this, we cultured and sequenced eight strains representing the significant phylogenetic diversity of the genus using long-read, short-read, and Hi-C DNA sequencing, alongside gene annotation and RNA sequencing. Comparative genomic analyses reveal significant variation in gene content and genome structure across *Blastocystis*. Notably, three strains from herbivorous tortoises, phylogenetically distant from human subtypes, have markedly larger genomes with longer introns and intergenic regions, and retain canonical stop codons absent in the human-associated strains. Despite these genetic differences, all eight isolates exhibit gene losses linked to the reduced cellular complexity of *Blastocystis*, including losses of cilia and flagella genes, microtubule motor genes, and signal transduction genes. Isolates from herbivorous tortoises contain higher numbers of plant carbohydrate-metabolizing enzymes, suggesting that, like gut bacteria, these protists ferment plant material in the host gut. We find evidence that some of these carbohydrate-metabolizing enzymes were horizontally acquired from bacteria, indicating that horizontal gene transfer is an ongoing process in *Blastocystis* that has contributed to host-related adaptation. Together, these results highlight substantial genetic and metabolic diversity within the *Blastocystis* genus, indicating that different lineages of *Blastocystis* have varied ecological roles in the host gut.

[Supplemental material is available for this article.]

The vertebrate gut is host to a diverse ecosystem of bacteria, archaea, viruses, and microbial eukaryotes. This diverse microbial community has broad impacts on the physiology and development of the host. Gut microbes can metabolize compounds that are not digestible by the host, providing access to previously inaccessible nutrients (Yadav et al. 2018). Gut microbes also influence the host's immune system and impact host health through their metabolic byproducts (Sommer and Bäckhed 2013). The microbiome's composition, which is influenced by diet, physiology, and the host immune system, varies substantially across vertebrate animals (Godoy-Vitorino et al. 2012; David et al. 2014; Thorman et al. 2023).

Compared to bacteria, substantially less is understood about microbial eukaryote impacts on host physiology and the gut ecosystem, despite the prevalence and diversity of gut microbial eukaryotes across vertebrates (Nash et al. 2017; del Campo et al. 2020). The protist *Blastocystis* is the most prevalent eukaryotic microorganism in the human gut, found in 10%–50% of industrialized populations and at higher prevalence in non-industrialized

communities (Scanlan and Marchesi 2008; Scanlan and Stensvold 2013; Scanlan et al. 2014; Khaled et al. 2020; Asnicar et al. 2021; Jinatham et al. 2021). Beyond humans, *Blastocystis* colonizes a wide range of animals including other mammals, birds, reptiles, fish, amphibians, and insects (Boreham and Stenzel 1993; Yoshikawa et al. 2016; Gantois et al. 2020). *Blastocystis* is a genetically diverse genus, with strains adapting to varied gut environments across different host species (Stensvold et al. 2007). Its presence is associated with positive health outcomes in humans, including lower levels of gut inflammation and metabolic health (Nieves-Ramírez et al. 2018; Asnicar et al. 2021; Piperni et al. 2024). However, very little is understood about how *Blastocystis* contributes to the gut environment and interacts with other gut microbiota.

*Blastocystis* belongs to the Opalinata lineage of stramenopiles, a group of protists that are obligate animal gut commensals (Kostka 2017). Unlike most stramenopiles, *Blastocystis* is non-motile, lacks flagella or surface hairs, and grows predominantly as a round cell with a large central vacuole (Zierdt 1988). The *Blastocystis* genus contains numerous genetically distinct groups categorized into

**Corresponding author:** [katherine.pollard@gladstone.ucsf.edu](mailto:katherine.pollard@gladstone.ucsf.edu)

Article published online before print. Article, supplemental material, and publication date are at <https://www.genome.org/cgi/doi/10.1101/gr.279080.124>. Freely available online through the *Genome Research* Open Access option.

© 2025 Lind et al. This article, published in *Genome Research*, is available under a Creative Commons License (Attribution-NonCommercial 4.0 International), as described at <http://creativecommons.org/licenses/by-nc/4.0/>.

subtypes based on polymorphism in the 18S rRNA gene. Thus far, 40 distinct subtypes have been proposed, and this number is continuing to expand (Stensvold and Clark 2020; Santin et al. 2024). To date, strains from three axenic lab-cultured subtypes (ST1, ST4, and ST7), all of which are subtypes observed in humans, have been sequenced, annotated, and deposited in public databases (Denoeud et al. 2011; Gentekaki et al. 2017). Although these subtypes span a narrow range of the *Blastocystis* phylogenetic diversity, they have very different genomes and gene contents (Gentekaki et al. 2017). These genomes have either gapped scaffolds (ST7) or highly fragmented non-contiguous genome assemblies (ST1, ST4), limiting the ability to determine synteny between subtypes, and two genomes were annotated without consideration for the unique *Blastocystis* phenomenon where a portion of genes lack DNA-encoded termination codons. Thus, we lack highly complete and well-annotated genomes necessary for establishing cases of gene loss, horizontal transfer, and sequence evolution so that functional repertoires can be associated with strain diversification.

Like most host-associated eukaryotes, *Blastocystis* grows best in the presence of other microbiota. Establishing robust axenic cultures of intestinal protists including *Blastocystis* is laborious and often either fails to remove all microbial contaminants or results in the death of the protist (Zierdt and Williams 1974; Tan 2008). However, removing sources of microbial contamination is important for eukaryotic genome assembly via short-read sequencing (Gough et al. 2020). As a result, genome sequencing for *Blastocystis* and other intestinal protists has been limited to axenic cultures (Keeling et al. 2014; Gough et al. 2020). To overcome this barrier, we establish high-quality and contamination-free genomes from xenic cultures of *Blastocystis* grown together with other microbes present in the original sample by using long-read Nanopore and Hi-C sequencing technologies coupled with short reads and metagenomic assembly techniques to establish genomes of *Blastocystis* strains that are grown together with other microbes. The longer read length of Nanopore sequencing helps span repetitive regions, resulting in greater contig length and fewer misassemblies, and has been successfully applied to assembling bacterial metagenomes (Moss et al. 2020). Hi-C sequencing, which captures spatial interactions between DNA fragments, can further improve genome assembly by correcting misassemblies and scaffolding contigs (Šimková et al. 2024). By combining these technologies with metagenomic assembly techniques, we were able to generate nearly complete *Blastocystis* genomes without the need for axenic culturing. This approach allows us to investigate the full genetic diversity of *Blastocystis*, even in the presence of other microbes, and to assemble highly contiguous genomes that were previously difficult to obtain.

Here, we applied this hybrid sequencing strategy to eight *Blastocystis* strains, five isolated from humans and three isolated from the herbivorous tortoise *Testudo horsfeldii*. These isolates, five of which are xenic, containing other microbes present in the original sample, and three of which are axenic, span the phylogenetic diversity of the *Blastocystis* genus, enabling us to investigate *Blastocystis* evolution and determine how *Blastocystis* has adapted to thrive in animal hosts with different diets, physiologies, and resident microbiota. Our highly contiguous and complete genomes allowed us to investigate patterns of genome evolution within and between subtypes and to compare the genus to related protists. This work demonstrates how high-quality genome assemblies can be created from xenic protist cultures by combining deep long-read sequencing with metagenomic

assembly techniques, enabling rigorous comparative genomic analyses.

## Results

### Capturing *Blastocystis* diversity

To investigate the evolution of the *Blastocystis* genus, from its initial divergence through its later diversification, we sequenced eight diverse *Blastocystis* strains. Strains were cultured anaerobically on egg media overlaid with a balanced salt solution and 25% heat-inactivated horse serum. Five of these strains correspond to three different previously defined “subtypes” (genetically similar groups historically identified in mammalian and avian species [Stensvold and Clark 2020]). These five strains were originally cultured from human fecal samples and were obtained from the American Type Culture Collection. These human isolated strains correspond to three of the four most prevalent *Blastocystis* “subtypes” (Beghini et al. 2017), genetically similar groups historically identified in mammalian and avian species (Stensvold and Clark 2020): two subtype (ST) 1 (Nandll, JDR), two ST3 (DL, NMH), and one ST4 (BT1). The remaining three strains were isolated from companion animal tortoises: two from different individuals of the domestic Russian tortoise species *Testudo horsfeldii* (Rus-B, Rus-S), and one from a Hermann’s tortoise *Testudo hermanni* (Hermann’s). We performed comparisons of the 18S rRNA gene of these four strains to other *Blastocystis* strains, finding that the tortoise isolates were distantly related to the human isolates and do not belong to a described mammalian or avian subtype (Fig. 1A; Supplemental Table S1). The closest related named subtypes to the tortoise isolates are ST15, which has been described in non-human primates, and ST28, which has been described in birds (Fig. 1A; Alfellani et al. 2013; Maloney and Santin 2021). Analysis of all eight cultures by light microscopy revealed predominantly vacuolar *Blastocystis* cells, containing a large central vacuole and a thin peripheral ring of cytoplasm. Although *Blastocystis* have been observed to adopt a variety of morphologies, vacuolar morphologies dominate cultured samples (Fig. 1B).

To explore how the *Blastocystis* genus has emerged and diversified, we compared the *Blastocystis* genomes generated in this work to those of two other sequenced stramenopiles: *Cafeteria burkhardae*, a free-living heterotrophic marine flagellate (Hackl et al. 2020), and the recently sequenced *Proteromonas lacertae*, a reptile gut commensal closely related to *Blastocystis* (Záhonová et al. 2023). These organisms are the closest relatives to *Blastocystis* that have sequenced genomes. Genome comparisons allowed us to reconstruct three evolutionary transitions that have occurred during stramenopile evolution: the transition from a free-living aquatic lifestyle to an anaerobic lifestyle inside the animal gut (comparing *Cafeteria* to *Blastocystis*/*Proteromonas*), the change in cell morphology from heterokont flagellate to aflagellate, spherical cells (comparing *Cafeteria*/*Proteromonas* to *Blastocystis*), and adaptations to different animal hosts (comparing *Blastocystis* tortoise to *Blastocystis* human) (Fig. 1B).

### Contiguous and complete *Blastocystis* genomes

We prepared high-quality, high molecular weight DNA, as well as RNA, from the eight *Blastocystis* cultures. DNA was sequenced with Nanopore long-read technology. Short-read DNA and RNA sequencing was also performed for assembly polishing and gene annotation. Hi-C data were additionally generated to help resolve scaffolds for one strain (ST4-BT1), although they resulted in only

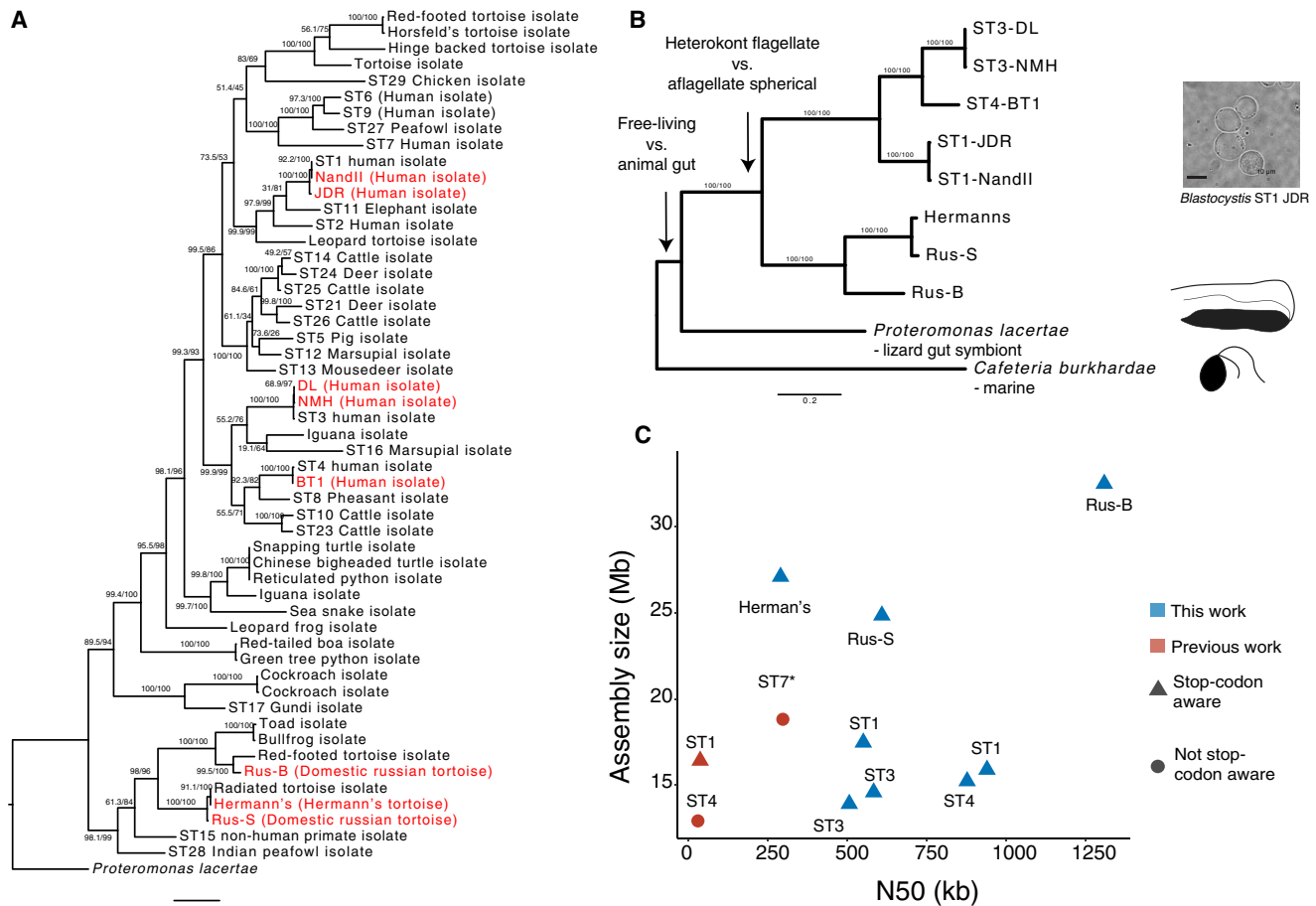


**Figure 1.** Phylogenetic relationships and genome assembly characteristics of *Blastocystis*. (A) 18S rRNA maximum likelihood (ML) phylogeny of *Blastocystis* subtypes, with *Proteromonas lacertae* as an outgroup. Support values are 1000 replicates of ultrafast bootstrap and SH-aLRT tests (Guindon et al. 2010; Hoang et al. 2018). Strains in red were sequenced in this study. (B) 13-gene concatenation ML phylogeny for all strains and species with sequenced genomes used in this study. Important evolutionary transitions are highlighted. Images represent cellular morphology of *Cafeteria burkhardae*, *Proteromonas lacertae*, and *Blastocystis*. (C) Assembly statistics of *Blastocystis* strains sequenced in this work compared with previously sequenced and annotated genomes. Stop-codon aware and not stop codon aware designations refer to gene annotation methodologies that take into consideration that *Blastocystis* genes can lack stop codons or do not consider this, respectively. The ST7 N50 is a gapped scaffold N50 generated with Sanger sequencing scaffolding.

modest improvements to the final assembly. Non-eukaryotic sequence was detected via multiple methods and excluded from final assemblies (see Methods, “Genome assembly and decontamination”). We additionally validated that our genomes were not contaminated by bacterial sequence by determining that genes with high sequence similarity to bacterial genes arose from polyadenylated eukaryotic transcripts (Supplemental Table S2) (see Methods, “Gene contamination and horizontal gene transfer screens”).

This combination of sequencing technologies enabled us to generate highly contiguous genomes for all six subtypes. The N50 of these assemblies ranged from 289 kb to 1.3 Mb, achieving a much higher assembly quality than currently available *Blastocystis* genome data sets in NCBI (median: 37 kb) (Table 1; Fig. 1C). We used the BUSCO pipeline to estimate genome completeness based on presence and absence of single-copy universal eukaryotic genes (Manni et al. 2021). BUSCO completeness estimates ranged from 42% to 61.2%, similar to BUSCO completeness results of previously sequenced *Blastocystis* isolates and related species (Table 1; Fig. 1C). These values likely underestimate the true

completeness, because BUSCO is known to have poorer performance in protists relative to plants, animals, and fungi (Saary et al. 2020). Nonetheless, the consistent recovery of a similar fraction of BUSCO genes across stramenopile genomes indicates comparable completeness. It is therefore striking that the sequenced *Blastocystis* strains showed substantial variability in genome size, from 14.0 to 32.2 Mb. Strains in the same subtype exhibited similar lengths: ST3 isolates were 14.0 and 15.3 Mb, and ST1 isolates were 17.2 and 16.0 Mb in size. In contrast, the genomes of the three tortoise isolates were ~1.5 to 2 times larger than human isolates, ranging from 26.0 Mb to 33.3 Mb.

Previous genome sequencing studies have raised questions about the ploidy of *Blastocystis* and found evidence of segmentally duplicated blocks of genes. With the highly contiguous genomes and multiple isolates of individual subtypes here, we investigated questions of ploidy and conservation of synteny both within *Blastocystis* subtypes and across the genus. *k*-mer frequency-based analysis using GenomeScope (Ranallo-Benavidez et al. 2020) demonstrated a strong diploid signal in all *Blastocystis* isolates, with limited evidence for aneuploidy or polyploidy. We found that strains

**Table 1.** Genome assembly statistics for all genomes used in this study

Species	Strain	Subtype	Source	Citation	Scaffolds (#)	Size (Mb)	N50 (kb)	GC content (% GC)	BUSCO content <sup>a</sup>	Protein-coding genes
<i>Blastocystis</i> sp.	JDR	1	Human	This study	114	17.5	550	54.5%	61.2%	7891
<i>Blastocystis</i> sp.	NandII	1	Human	This study	54	16.0	939	54.7%	61.2%	7157
<i>Blastocystis</i> sp.	NMH	3	Human	This study	36	14.6	582	51.3%	58.0%	6571
<i>Blastocystis</i> sp.	DL	3	Human	This study	56	14.0	506	51.6%	55.7%	6154
<i>Blastocystis</i> sp.	BT1	4	Human	This study	34	15.3	882	39.4%	57.6%	7421
<i>Blastocystis</i> sp.	Rus-B	N/A	Russian tortoise	This study	33	33.3	1323	23.1%	43.2%	8547
<i>Blastocystis</i> sp.	Rus-S	N/A	Russian tortoise	This study	258	26.1	505	21.8%	42.0%	8501
<i>Blastocystis</i> sp.	Hermanns	N/A	Hermann's tortoise	This study	229	27.1	289	21.5%	42.4%	8349
<i>Blastocystis</i> sp.	WR1	4	Laboratory Wistar rat	No publication	1301	12.9	30	39.5%	56.5%	5707
<i>Blastocystis</i> sp.	NandII	1	Human	Gentekaki et al. 2017	580	16.5	79	55.0%	61.1%	6544
<i>Blastocystis</i> sp.	Singapore	7	Human	Denoeud et al. 2011	54	18.8	901 <sup>b</sup>	45.0%	52.2%	6020
<i>Proteromonas lacertae</i>	LA	N/A	Sand lizard	Záhonová et al. 2023 <sup>c</sup>	1447	52.2	93	27.0%	62.7%	23,189
<i>Cafeteria burkhardae</i>	BVI	N/A	Environmental	Hackl et al. 2020	169	36.3	465	70.0%	54.9%	8591

<sup>a</sup>BUSCO version 5.6.1 with eukaryote\_odb10 lineage, metaeuk genome mode.

<sup>b</sup>Gapped scaffold N50.

<sup>c</sup>Citation for genome only. Annotations not publicly available and generated for comparative genomics in this work.

within ST3 and within ST1 were highly syntenic (Supplemental Fig. S1). However, synteny between subtypes was much lower, broadly following the relatedness between strains based on 18S sequences.

We used a hybrid method of de novo gene prediction and RNA transcript evidence to annotate *Blastocystis* genes (see Methods, “Genome assembly and decontamination”). Because a substantial fraction of genes in *Blastocystis* ST1 and ST7 do not have DNA-encoded stop codons (Klimeš et al. 2014; Gentekaki et al. 2017) (discussed below), open reading frame-based gene predictions from DNA sequence are inaccurate. Leveraging our RNA sequencing data, we were able to generate a comprehensive gene annotation for each *Blastocystis* genome that was able to accurately call genes lacking stop codons (see Methods, “Gene annotation”). Similar approaches were taken for one previously sequenced ST1 genome (Gentekaki et al. 2017), but published *Blastocystis* genomes for ST4 and ST7 were not annotated with these approaches, leading to incorrect gene annotations. For the *Blastocystis* strains sequenced in this study, the number of genes per *Blastocystis* genome sequenced in this work ranged from 6154 to 8547 (Table 1). Protein amino acid identity (AAI) across 753 single-copy orthologs was almost identical between strains of the same subtype (99%–100% AAI for both ST1 and ST3) and decreased to 65%–75% between human *Blastocystis* isolates from different subtypes and to 40%–42% between human and tortoise isolates (Supplemental Fig. S2). Tortoise isolates had lower pairwise AAI than human isolates, with the most distantly related strains in the tortoise-associated clade having a protein identity of 56% AAI for the same 753 orthologs, suggesting substantial genetic distance within this group.

### Genomic diversity within *Blastocystis*

When we compared sequenced *Blastocystis* genomes, we found substantial variation in the genomes between human *Blastocystis*

isolates and the tortoise-associated clade, including genome size. Whereas the tortoise *Blastocystis* isolate genomes are ~1.5×–2.4× larger than the human isolate genomes, this difference is not reflected in protein-coding gene content, suggesting that non-genic regions are driving the difference in genome size. We sought to determine why the genomes of *Blastocystis* isolates in the tortoise-associated clade were larger than the genomes of the *Blastocystis* human isolates.

We found little difference in transposable element presence across *Blastocystis*, which ranges from 4.2% to 6.7% of the genome in the human isolates and 5.6% to 7.5% of the genome in the tortoise isolates. However, we did observe an increase in low-complexity regions in the tortoise isolates, comprising 0.02%–1.4% of the human isolate genomes and 11.8%–12.7% of the tortoise isolate genomes (Supplemental Table S3). This increase in low complexity regions does not explain the difference in genome size; if these regions are removed, the tortoise isolates remain 1.3×–2.1× larger than the human isolates. These low-complexity regions may be related to the overall lower GC content of the tortoise isolates, which ranges from 21% to 23% in tortoise isolates to 39% to 55% in human isolates (Table 1).

As repetitive elements did not explain differences in genome size, we investigated differences in other genomic features. We found that the almost all introns in human ST1, ST3, and ST4 *Blastocystis* are exactly 30 bp long, in agreement with previous estimates of intron size in *Blastocystis* ST1 and ST7 (Denoeud et al. 2011; Gentekaki et al. 2017). However, introns in the tortoise isolates are longer and more variable in length (Fig. 2A). We additionally found that the intergenic spaces between genes are much longer in the tortoise *Blastocystis* isolate than in human isolates (Fig. 2B). The median intergenic length in the tortoise isolates ranges from 645 to 719 bp, whereas the median intergenic length

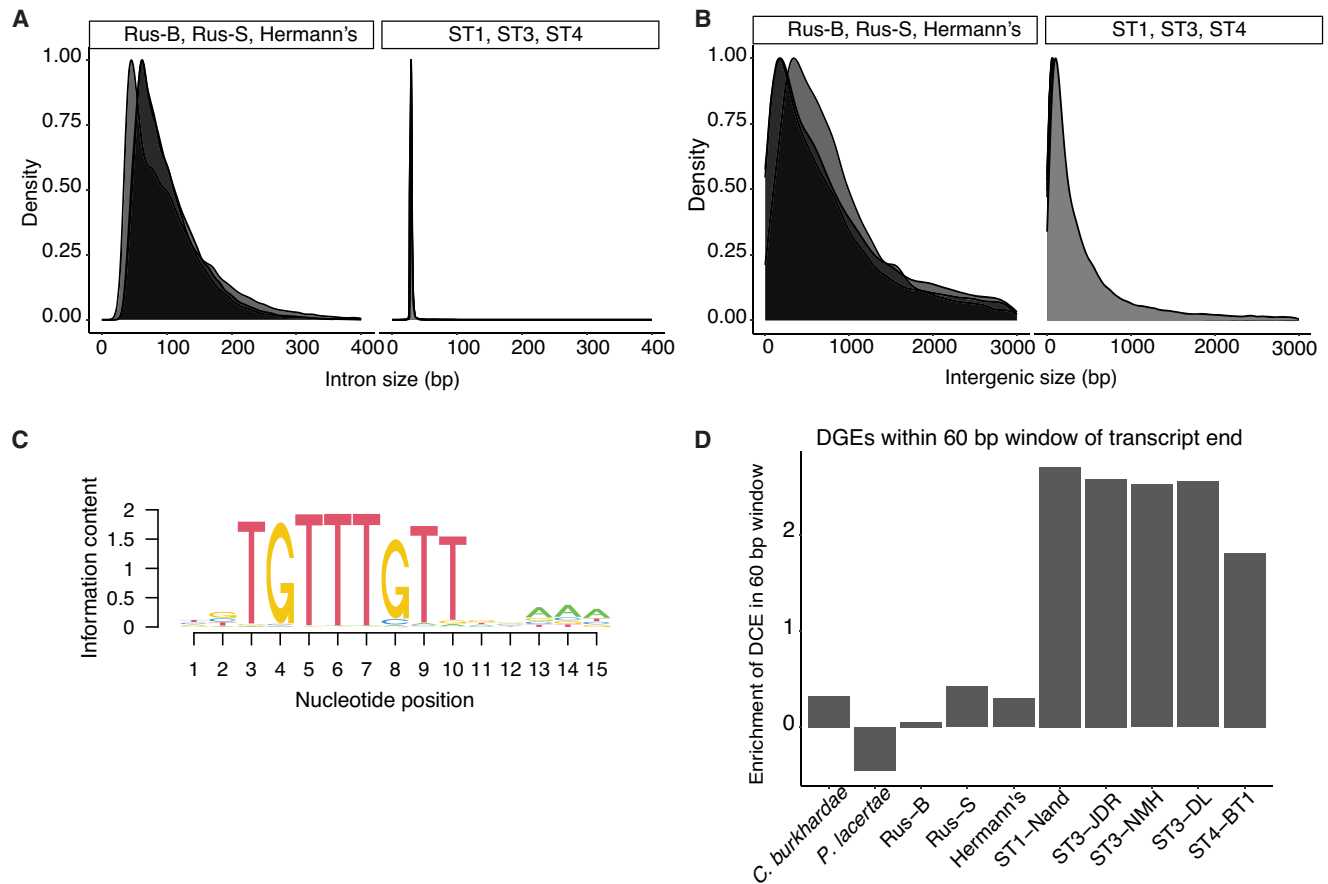


**Figure 2.** Genomic features differ across *Blastocystis* strains. (A) Intron lengths and (B) intergenic lengths in tortoise isolates (left) and human isolates (right). (C) Sequence motif enriched adjacent to transcript ends in ST1, ST3, and ST4. Motif generated with STREME (Bailey 2021). This motif is referred to as “downstream gene element” (DGE). (D) Enrichment (log[observed/expected]) of transcripts with downstream conserved element within 30 bp upstream of or downstream from transcript end, normalized by expected DGE occurrence given GC content.

in the human isolates ranges from 137 to 186 bp. Intergenic lengths in the human isolates can frequently be extremely small, only spanning tens of base pairs (Fig. 2B). Together, the total amount of DNA spanned by introns and intergenic regions is 13.9–16.5 Mb in the tortoise *Blastocystis* isolates, whereas these regions span only 3.7–5.7 Mb in human *Blastocystis* isolates. Considered together, the larger introns and intergenic distance in the tortoise isolates explain the difference in their genome sizes relative to the human isolate.

#### Loss of stop codons is not universal in *Blastocystis*

In addition to genome size and gene density, we found surprising differences in how genes are encoded in the genome across *Blastocystis*. In *Blastocystis* ST1 and ST7, a fraction of protein coding genes (15% for ST7 and 26% for ST1) lack canonical DNA-encoded termination codons (Klimeš et al. 2014; Gentekaki et al. 2017). A proposed mechanism for translation of these genes is that the translational machinery instead uses a U or a UG sequence in mRNA, along with one or two adenines from the poly(A) tail, to generate UAA and UGA on-the-fly stop codons (Klimeš et al. 2014). Additionally, these genomes have a highly conserved motif (downstream gene element, or DGE) roughly 5 bp downstream from transcription stop sites of most genes. These sequences are hypothesized to direct 3' mRNA cleavage and polyadenylation fac-

tors to the pre-mRNA (Klimeš et al. 2014; Gentekaki et al. 2017). In a scenario where the DGE is sufficient for 3' mRNA cleavage, the loss of DNA-encoded stop codons is driven by relaxation of the selection pressure maintaining them.

We investigated all *Blastocystis* isolates for the DGE motif, finding enrichment downstream of protein coding genes in human-isolated *Blastocystis* strains but not downstream from tortoise-isolated *Blastocystis* strains or other stramenopiles (Fig. 2C, D). We additionally found no evidence of transcripts lacking stop codons in the tortoise-associated *Blastocystis* clade, suggesting that the unique transcriptional cleavage machinery described in *Blastocystis* ST1, ST4, and ST7 (Klimeš et al. 2014; Gentekaki et al. 2017) evolved after the divergence of the tortoise- and the human-associated clades sequenced here.

#### Gene losses related to cell morphology and signaling unite the *Blastocystis* genus

Despite the substantial variation in genome diversity for all *Blastocystis* strains sequenced here, the strains share the typical spherical, non-motile *Blastocystis* cell morphology lacking flagella. We find that all *Blastocystis* isolates are united by substantial gene loss related to this morphological change across multiple functional categories. All *Blastocystis* isolates have lost nearly all cilia- and flagella-related genes (Fig. 3; Supplemental Tables S4, S5). They

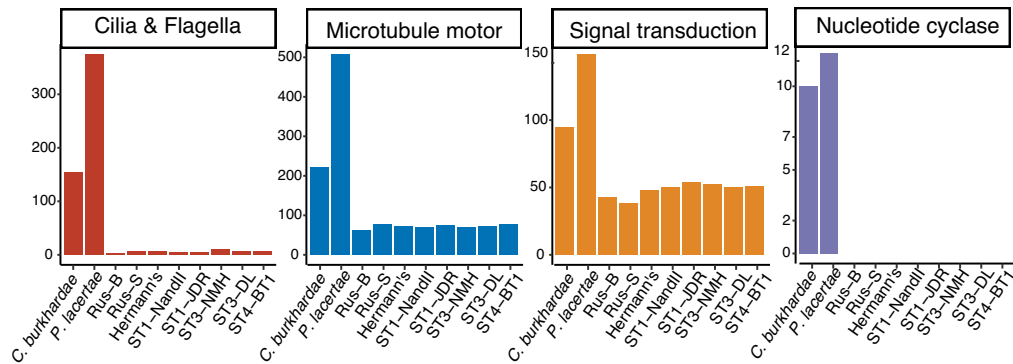


**Figure 3.** Gene families lost or reduced in all *Blastocystis* strains. See Supplemental Table S2 for GO categories and InterPro domains used for defining categories.

have also undergone substantial reduction of dynein and kinesin microtubule motor proteins, retaining what is likely the minimal amount of motor proteins required for intracellular transport. This agrees with recent analyses showing reduction in these gene families in human-associated *Blastocystis* subtypes (Záhonová et al. 2023) and extends that observation by demonstrating that these losses unite the genus. In addition, we find that *Blastocystis* isolates have lost nucleotide cyclases and many genes related to signal transduction (Fig. 3; Supplemental Tables S4, S5). As cilia are major mediators of cell signaling that use cyclic nucleotides as intermediaries (Johnson and Leroux 2010), the loss of cilia in *Blastocystis* likely corresponds to the loss of nucleotide cyclases and reduction in signal transduction related genes. Thus, our sequencing of diverse *Blastocystis* strains provides strong evidence that the flagella-free morphology and associated gene losses evolved in the common ancestor of the *Blastocystis* genus.

#### Lineage-specific genes reveal specialization within the *Blastocystis* genus

We find multiple differences in gene content in between *Blastocystis* isolates that likely reflect their ecological niche. All strains in the herbivorous tortoise-associated *Blastocystis* clade have a larger number of genes involved in plant carbohydrate degradation than the human-associated subtypes. We found five carbohydrate-degrading enzyme families that were either uniquely present in the tortoise isolates or in higher copy numbers, four of which are specific to degrading plant carbohydrates. This includes polygalacturonases,  $\beta$ -D-xylosidases,  $\alpha$ -L-arabinofuranosidases,  $\alpha$ -L-fucosidases,  $\alpha$ -L-rhamnosidases, arabinogalactanases, and  $\beta$ -hexosaminidases (Fig. 4). Polygalacturonase is a pectinase that degrades plant cell walls; it was originally characterized in plants but is also present in phytopathogenic microbes and in bacterial members of ruminant microbiomes (De Lorenzo and Ferrari 2002; Deng et al. 2023).  $\beta$ -D-xylosidases and  $\alpha$ -L-ara-

binofuranosidases are both critical enzymes for degrading xylan, a carbohydrate specific to plant hemicellulose (Yang et al. 2004; Lagaert et al. 2014). The GH154 arabinogalactanase gene family that is present only in the tortoise-associated clade was recently characterized in the gut bacteria *Bacteroides thetaiotamicron* as acting on plant-derived arabinogalactan glycans (Cartmell et al. 2018). Finally,  $\alpha$ -L-rhamnosidases are active on a wide variety of polysaccharide residues produced by plants and bacteria (Guillotin et al. 2019). Together, the presence of multiple plant-specific carbohydrate-digesting enzymes in the herbivorous tortoise-associated clade strongly suggests that, like the bacterial microbiota, *Blastocystis* utilize dietary plant fiber as a carbon source and participate in the hindgut plant fiber fermentation that is characteristic of herbivorous tortoises (Stevens and Hume 1995).

#### Ongoing horizontal gene transfer from bacteria in the *Blastocystis* genus

Horizontal gene transfer from bacteria has played an important role in *Blastocystis* evolution, particularly with respect to survival

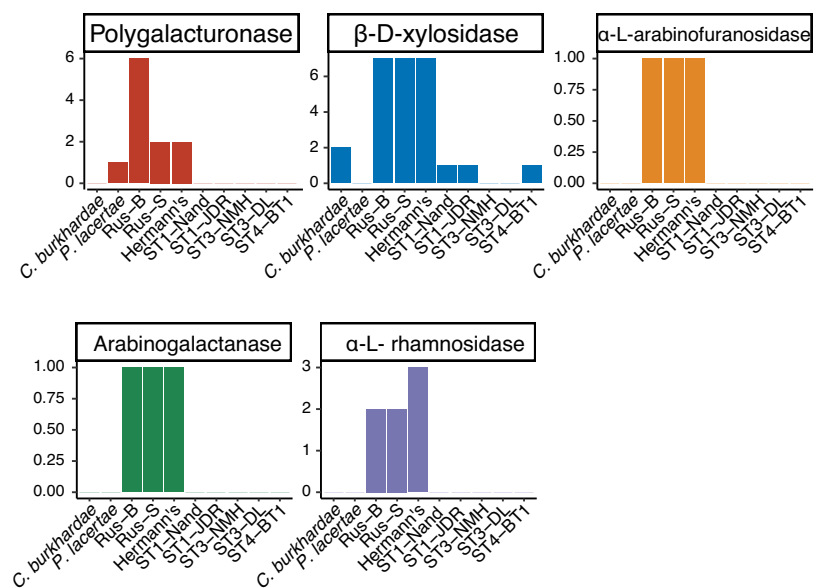


**Figure 4.** Clade-specific gene family expansions across *Blastocystis*, identified with InterProScan.

in an anaerobic environment (Eme et al. 2017). With high-quality genomes of *Blastocystis* isolates that span the genus, in combination with the genomes of other stramenopiles, we can estimate times of these transfer events. We re-analyzed HGT events into ST1 previously identified in Eme et al. (2017) and additionally screened all sequenced *Blastocystis* genomes for evidence of additional transferred genes (see Methods, “Gene contamination and horizontal gene transfer screens”).

Previous analysis of *Blastocystis* ST1, ST4, and ST7 genomes identified 74 horizontal transfer events in *Blastocystis* ST1 from bacteria (Eme et al. 2017). We were able to confidently identify orthologous genes for 66 of these genes (Supplemental Table S6), of which 29 genes had strong phylogenetic support for horizontal gene transfer from bacteria to eukaryotes, 17 genes lacked strong phylogenetic support for horizontal gene transfer, and the remaining 20 genes were ambiguous. In most ambiguous cases, the *Blastocystis* genes were either sister to an entirely bacterial tree, there were too few orthologs in the NR database to construct a gene tree, or the placing of the *Blastocystis* sequences on the phylogeny lacked strong support.

We additionally screened all genomes sequenced for new cases of HGT. To minimize the impact of potential genome contamination, we limited this screen to genes that were expressed in our RNA-seq data, were shared in more than one *Blastocystis* genome, and were flanked by unambiguously eukaryotic sequence to (see Methods). We found 13 newly identified HGT cases, six which are unique to the tortoise-associated *Blastocystis* lineage (Fig. 5A).

Two of the six tortoise-unique transfers are glycoside hydrolase genes, alpha-L-rhamnosidase and arabinogalactanase, that are uniquely expanded in this lineage and not present in the human *Blastocystis* isolates. The remaining transfers are two GNAT family N-acetyltransferases, a cold-shock protein, and a SMI1/KNR4 family protein (Supplemental Table S7).

The alpha-L-rhamnosidase gene family cleaves alpha-L-rhamnose from a large diversity of molecules and is present across the tree of life. This gene is present in two copies in Rus-B and Rus-S and three copies in Hermann's and is not present in any human *Blastocystis* isolates or in *P. lacertae*. Two genes with the alpha-L-rhamnosidase Interpro domain were present in the

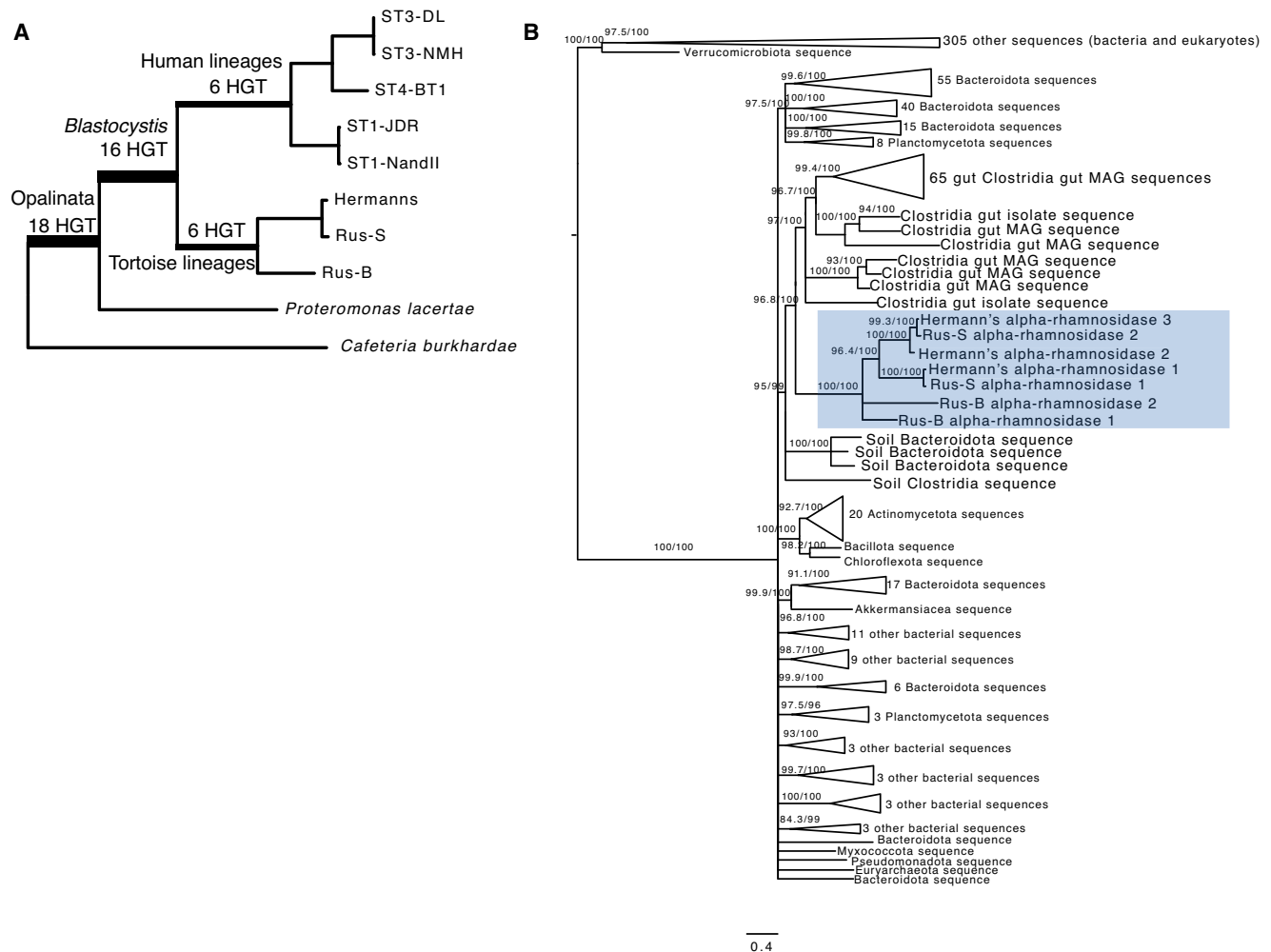


**Figure 5.** Horizontal gene transfer across *Blastocystis* evolution. (A) Estimated time of transfer for 40 horizontally transferred genes in *Blastocystis* shared between more than one species or strain. These data include previously identified and validated cases originally identified in Eme et al. (2017) and newly identified transfer events. (B) Gene phylogeny of tortoise isolate alpha-rhamnosidase genes and 588 homologous proteins. Support values indicate 1000 replicates of SH-aLRT test and ultrafast bootstraps (UFboot). Branches with support values <95 for UFboot or <80 for SH-aLRT are collapsed.

*C. burkhardae* genome. We constructed a gene phylogeny of the *C. burkhardae* genes and the tortoise genes together with 588 homologous genes retrieved with a sequence search of the *Blastocystis* and *C. burkhardae* sequences against the clustered NCBI NR database (see Methods). The gene phylogeny was separated into two fully supported clades, one with the *C. burkhardae* sequences, eukaryotic sequences from protists and rotifers, and some bacterial sequences, and the other with bacterial sequences and the *Blastocystis* sequences (Fig. 5B). The tortoise sequences grouped together with sequences from gut isolates and gut metagenome-assembled genomes in the Clostridia bacterial class, which contains prevalent members of the animal gut microbiota. Thus, the *Blastocystis* tortoise lineage likely acquired this carbohydrate-degrading enzyme from Clostridia bacteria present in the gut microbiome, suggesting a gut-specific function.

The other horizontally transferred carbohydrate gene in the tortoise *Blastocystis* lineage is within the recently described GH154 glycoside hydrolase gene family, characterized in *Bacteroides thetaiotamicron* as acting on plant-derived arabinogalactan glycans (Cartmell et al. 2018). This gene family is present exclusively in the tortoise *Blastocystis* isolates and not found in any other *Blastocystis* isolates or any other stramenopile genomes. A sequence search for the tortoise *Blastocystis* genes against the clustered NCBI NR database did not return any eukaryotic hits. A gene phylogeny of all bacterial homologs and the tortoise *Blastocystis* genes shows the tortoise *Blastocystis* genes group together with bacteria in the *Bacteroidota* (syn. *Bacteroidetes*) phylum (Supplemental Fig. S3).

We did not find strong evidence that the other three carbohydrate gene families uniquely present or expanded in the tortoise *Blastocystis* lineage were horizontally acquired from bacteria. Homologs to the polygalacturonase gene were all eukaryotic. Although the evolutionary history of this gene is likely complex as most homologs were within Streptophyta, it was not horizontally acquired from bacteria.  $\beta$ -D-xylosidase and  $\alpha$ -L-arabinofuranosidase both appeared to have complex evolutionary histories but without conclusive evidence of horizontal gene transfer. Specifically, several of the  $\beta$ -D-xylosidase genes in the tortoise lineages had no eukaryotic homologs, but a gene phylogeny of all  $\beta$ -D-xylosidase genes including the human isolates did not yield a well-supported branch of the tortoise genes nested within bacteria. Similarly, the  $\alpha$ -L-arabinofuranosidase gene had both bacterial and eukaryotic homologs, but there was not strong support for the placement of the *Blastocystis* sequences on this phylogeny either with the eukaryotic sequences or with the bacterial sequences.

Together, these results indicate that horizontal gene transfer played a major role in all evolutionary transitions investigated in this work: at the evolutionary transition from free-living to gut symbiont, in the *Blastocystis* genus broadly, and is an ongoing method of genetic diversification in this organism.

## Discussion

The stramenopile protist *Blastocystis* is the most prevalent protist in the human gut and is widespread throughout vertebrates. Here, we present contiguous and complete genomes of eight *Blastocystis* strains, five isolated from humans and three from herbivorous tortoises. Long-read sequencing coupled with metagenomic assembly techniques enabled us to assemble three of these genomes from xenic cultures containing microbes present in the original sample, which has been technically infeasible with standard short-read approaches. Comparative genomic anal-

yses between these *Blastocystis* genomes alongside other closely related stramenopiles revealed evolutionary changes that the *Blastocystis* genus has undergone to colonize a wide variety of animal guts.

The herbivorous tortoise isolates of *Blastocystis* diverged substantially from the human isolated *Blastocystis* and have many genomic features not seen in the human isolates. We found substantial changes in genome size, with human isolates possessing significantly shorter introns and intergenic regions than the tortoise isolates and substantially lower GC content in tortoise isolates. The GC content of the tortoise isolates is substantially lower than the genomes of most sequenced stramenopiles; of the 299 stramenopiles with sequenced genomes deposited in the NCBI GenBank database (<https://www.ncbi.nlm.nih.gov/genbank/>), only three genomes have lower GC content.

It is not clear whether introns and intergenic regions have shrunk in size after the split of the tortoise-human isolates, or if they have lengthened along the tortoise lineage. Genomic streamlining is a frequently observed process in symbiotic and parasitic organisms (McCutcheon and Moran 2012; Leckenby and Hall 2015), and some parasitic eukaryotes have entirely or almost entirely lost introns (Wilihoeft et al. 2001; Wang et al. 2018). The phenomenon of intergenic and intron size shrinking in *Blastocystis* likely reflects this general process, but the unexpected differences between different host-associated *Blastocystis* isolates highlights that this is an ongoing evolutionary process that can proceed at different rates.

Despite these substantial differences in genomic streamlining, all *Blastocystis* isolates sequenced here have undergone loss of the same genes associated with the more complex flagellated cell morphology of other stramenopiles. *Blastocystis* isolates have lost nearly all cilia- and flagella-related proteins, substantially reduced the number of microtubule motor proteins, and have lost all nucleotide cyclases and many signal transduction-related genes. These changes unite all *Blastocystis* isolates, demonstrating shared biology across the genus despite large evolutionary distances and differences in genome structure between isolates.

We additionally find evidence consistent with host adaptation within *Blastocystis*. The *Blastocystis* strain isolated from herbivorous tortoises contained many carbohydrate-digesting enzymes not present in other *Blastocystis* isolates (Fig. 4). Two of these gene families were acquired via horizontal transfer from bacteria and, in one case, via horizontal transfer from bacteria that also colonize the animal gut. The presence of plant-specific carbohydrate-digesting enzymes suggests that, like some ciliates and many gut bacteria, *Blastocystis* may ferment plant carbohydrates, a critical element of energy homeostasis in predominantly plant-eating animals (Stevens and Hume 1995).

Although *Blastocystis* is widespread across vertebrates, there is limited evidence for co-phylogeny of *Blastocystis* subtypes with their host (Fig. 1). Instead, the *Blastocystis* phylogeny more closely resembles that of spore-forming gut bacteria (Moeller et al. 2016), with host switching as a common phenomenon. Because of the lack of strong co-phylogenetic signal, open questions remain about *Blastocystis* host association, including what the barriers to colonizing different hosts are and how multiple strains or subtypes (commonly termed “mixed infections”) are maintained, and will require a denser sampling of genomes across the *Blastocystis* tree of life. As human-associated *Blastocystis* subtypes are not monophyletic, understanding the biology of the protists that impact humans will require considering *Blastocystis* subtypes that are present in the guts of diverse vertebrate hosts and how these subtypes

function in different environments. Finally, the vast differences seen in the phylogenetically distinct tortoise *Blastocystis* isolates sequenced here compared to previous sequenced human-associated *Blastocystis* isolates highlight that substantial genetic diversity in this genus has yet to be explored.

Five of the eight *Blastocystis* strains sequenced in this work were grown in the presence of other microbes. Despite the challenges of generating highly contiguous and contamination-free genomes from mixed culture metagenomic sequencing, we successfully combined advances in deep long-read DNA sequencing and metagenomic assembly techniques to acquire high-quality genomes from xenic cultures. To address the challenge of annotating genes in genomes where stop codons are not universal, we utilized RNA-sequencing and state-of-the-art annotation pipelines. These two technical accomplishments were essential for enabling robust comparative genomic analyses of *Blastocystis* and its closest sequenced relatives. The strategy established in this study can be extended in future work to the many eukaryotic microbes that cannot be cultured axenically. The resulting genomes will fill critical gaps in our understanding of eukaryotic microbes and the evolution of this domain of life.

## Methods

### Strain cultivation

*Blastocystis* strains NandII (ATCC 50177), JDR (ATCC 50587), BT1 (ATCC 50608), DL (ATCC 50626), and NMH (ATCC 50754) were obtained from the American Type Culture Collection. The JDR strain was labeled as subtype 3 based on rRNA analysis, but 18S rRNA gene sequencing and subsequent genome sequencing revealed, in fact, that this strain belongs to subtype 1. All strains were isolated from human sources. Cultures were incubated under anaerobic conditions at 37°C on biphasic egg slant media overlaid with Locke's solution supplemented with 25% heat-inactivated horse serum (ATCC Medium 1671). Media was pre-reduced for 24 h before use. ST1 and ST4 strains were maintained in axenic culture, while ST3 and tortoise isolates were grown in xenic culture alongside other microbes present in the original samples. These xenic culture strains proved resistant to axenization.

*Blastocystis* strains from tortoises were isolated from fresh fecal material that was processed within 8 h of sampling. Fecal material was resuspended in sterile PBS, strained using a 70- $\mu$ m cell strainer, and centrifuged at 700g for 5 min at room temperature. The pellet was then washed three times with PBS before being resuspended in 80% Percoll. This was overlaid with 40% Percoll and centrifuged at 100g for 10 min at room temperature. Protists were removed from the top of the 40% Percoll layer, washed in PBS, and resuspended in pre-reduced growth medium.

### DNA extraction and sequencing

High molecular weight DNA was isolated from *Blastocystis* cultures with a modified CTAB-based protocol (adapted from McLay 2017) that minimizes polysaccharide contamination. *Blastocystis* cells were collected from cultures by pelleting with centrifugation at 800g for 5 min and snap frozen at -80°C. Frozen pellets were gently resuspended in two volumes of a high salt CTAB lysis buffer (100 mM Tris pH 8, 1.2 M NaCl, 10 mM EDTA, 4% CTAB, 1% PVP-40), and 200  $\mu$ g/mL RNase A and 200  $\mu$ g/mL Proteinase K were added before incubation at 60°C for 90 min. One volume of phenol:chloroform:isoamyl alcohol (25:24:1) was added, and samples were mixed end over end for 15 min. Samples were centrifuged at 17,000g for 10 min, and the upper aqueous layer was recovered.

Two additional extractions were performed with pure chloroform, recovering the upper aqueous layer each time. DNA was next precipitated with two volumes of a low salt CTAB precipitation buffer (100 mM Tris pH 8, 10 mM EDTA, 2% CTAB) by end over end rotation at 60°C for 2.5 h. DNA was pelleted by centrifugation at 17,000g for 20 min. DNA pellets were washed twice with 75% ethanol and resuspended in 10 mM Tris pH 8. Genomic DNA was further cleaned with 1.8 volumes of Ampure XP beads according to the manufacturer's protocol (Beckman Coulter). RNA was isolated from *Blastocystis* cultures with a TRIzol extraction following the manufacturer's protocols (Invitrogen).

Nanopore sequencing libraries for all human isolates and for the Rus-B strain were prepared using the Genomic DNA by Ligation protocol SQK-LSK109 (Oxford Nanopore Technologies) following the manufacturer's instructions, sequenced on a full FLO-MIN106D R9 flow cell on a MinION sequencer, and basecalled with Guppy version 5.0.16. Nanopore sequencing libraries for the Rus-S and Hermann's isolates were prepared using the SQK-LSK110 kit LSK109 (Oxford Nanopore Technologies), sequenced on a full R10.4.1 flow cell, and basecalled with Dorado version 0.5.3 (<https://github.com/nanoporetech/dorado>).

Short-read Illumina DNA and RNA libraries were prepared using the KAPA HyperPlus PCR-free and KAPA mRNA capture kits (Roche), respectively, following the manufacturer's instructions. RNA integrity and library fragment size distribution were quantified using a Bioanalyzer 2100 (Agilent). Illumina DNA and RNA libraries for all human *Blastocystis* isolates and for the Rus-S and Hermann's tortoise isolates were sequenced on an Illumina NextSeq 500 (Illumina), and libraries for the Rus-B tortoise isolate were sequenced on an Illumina MiSeq v3.

### Genome assembly and decontamination

Basecalled nanopore reads were assembled using Flye version 2.9.2 with the --meta option enabled (Kolmogorov et al. 2019, 2020). Assembly polishing was performed using four rounds of nanopore-read polishing using racon version 1.4.3 (Vaser et al. 2017), three rounds of Illumina DNA polishing using PolyPolish version 0.5.0 (Wick and Holt 2022), and one round of short-read polishing using POLCA as implemented in MaSuRCA version 4.0.9 (Zimin et al. 2013).

For the ST4 strain BT1, Hi-C data were generated using a Phase Genomics Proximo Hi-C 2.0 kit, and the Phase Genomics Proximo Hi-C genome scaffolding platform was used to create chromosome-scale scaffolds from the hybrid assembled genome. The Hi-C scaffolding resulted only in modest improvements to the original assembly quality; the number of scaffolds reduced from 45 to 34, and the assembly N50 improved to 882 from 876.

We used three different methods to separate eukaryotic, *Blastocystis*-originating sequence from other microbial sequences for xenic and axenic assemblies. For xenic assemblies, sequences were binned using MetaBAT 2 version 2.17.60 as a binning algorithm, taxonomically annotated using MetaEuk taxtocontig, and additionally annotated as likely eukaryotic or prokaryotic using EukRep (West et al. 2018; Kang et al. 2019; Levy Karin et al. 2020). For binning, short DNA sequencing reads were aligned to the polished assembly using minimap2 version 2.26-r1175 and summarized using the utility jgi\_summarize\_bam\_contig\_depths (Li 2018). Metaeuk taxonomy prediction was performed by running version 1f7d7023bdac3d46964ca380bef1b2848685501e, metaeuk easy-predict with mmseqs Swiss-Prot database build and metaeuk taxtocontig with the options "--majority 0.5 --tax-lineage 1 --lca-model 2". EukRep v0.6.6. was run in "balanced" mode.

Eukaryotic contigs were identified through a union of MetaEuk contigs annotated as eukaryotic, removing any not

identified as eukaryotic by EukRep. We found that MetaEuk was not able to identify *Blastocystis* contigs reliably at lower taxonomic levels than the superkingdom Eukaryota, which we validated by running the pipeline on existing NCBI genomes. Instead, any contigs that were annotated as eukaryotic were considered as potentially *Blastocystis* in origin. We cross-referenced these eukaryotic contigs with metabat bins, finding bins corresponding to eukaryotic sequence. In two cases, eukaryotic sequences that appeared to be *Blastocystis* in origin were split across two metabat bins, and these bins were combined. We removed any sequences from these bins that were annotated by MetaEuk as non-eukaryotic. We verified that these final cleaned bins corresponded to *Blastocystis* by BLASTing the NCBI RefSeq *Blastocystis* coding gene sequences against these bins. In several cases, we found bins that were annotated as eukaryotic but did not have any hits to *Blastocystis* coding sequences. These bins were discarded as likely originating from non-*Blastocystis* eukaryotic organisms in the culture.

We found that contigs containing ribosomal RNA genes were often not binned together with protein-coding genes, likely due to their highly repetitive nature and differences in DNA coverage. We searched for contigs containing 18S rRNA genes by BLASTing 18S rRNA genes against the full assembly. Contigs with full length and high percent identity hits to any *Blastocystis* 18S genes that were also annotated as eukaryotic by MetaEuk were included in final assemblies.

For axenic assemblies, sequences were not binned with MetaBAT 2, but MetaEuk and EukRep were performed as described above to identify potential contaminating sequences. This resulted in two contigs being removed from the BT1 assembly and no contigs being removed from Nand or JDR assemblies.

Genome completeness was determined with sequenced-based and gene-based approaches. For the sequence-based approach, we applied a *k*-mer frequency-based approach with GenomeScope v2.0 (Ranallo-Benavidez et al. 2020). Gene-based completeness was determined using BUSCO v5.6.1 with the lineage data set eukaryote\_odb10 in the genome mode (Manni et al. 2021). Synteny was plotted using odp (Schultz et al. 2023).

### Annotating repetitive elements

Repetitive elements in *Blastocystis* were annotated with a combination of RepeatMasker and RepeatModeler using the Dfam database version 3.8 (Smit et al. 2013; Flynn et al. 2020; Storer et al. 2021). Repetitive elements were predicted from all genomes with RepeatModeler version 2.0.5 with LTRStruct enabled. The predicted transposable elements from all *Blastocystis* genomes that had a putative predicted annotation were combined, and repetitive elements were tabulated in each genome with a combination of the custom repeat library created with RepeatModeler and the Dfam v3.8 database with RepeatMasker 4.1.7-p1.

### Gene annotation

*Blastocystis* genes occasionally do not encode stop codons, which confounds prediction via open reading frame and requires RNA-seq-based evidence (Klimeš et al. 2014; Gentekaki et al. 2017). Without consideration of lack of stop codons, common gene annotation errors include insertion of erroneous introns and combining adjacent genes. To accurately annotate the *Blastocystis* genomes, we created a pipeline that used a combination of de novo gene prediction with BRAKER3 and transcriptome assembly, combining all sets of gene models with Mikado (Venturini et al. 2018; Gabriel et al. 2024).

RNA-seq reads were aligned to assemblies with STAR version 2.7.11b (Dobin et al. 2013), with a minimum of three supporting reads required for each junction. Transcript assemblies were generated with StringTie version 2.2.3 (Pertea et al. 2015), which uses RNA-seq alignments against a genome to assemble transcripts. Because *Blastocystis* has very short intergenic regions, transcript assemblers can occasionally combine multiple transcripts into one. To address this, assembled transcripts were split if an exon had zero RNA-seq coverage. Assembled transcripts <100 bp long were discarded. To generate de novo gene predictions, braker version 3.0.8 was run with OrthoDB11 Eukaryota proteins as protein evidence and the aligned RNA-seq as transcript evidence (Kuznetsov et al. 2022; Gabriel et al. 2024). The Mikado transcript scoring file (available in code repository) was optimized to choose transcripts with strictly RNA-seq-supported introns but to prioritize genes containing stop codons so long as the intron boundaries were strictly supported.

### Functional annotation and orthology inference

Proteins from *Cafeteria burkhardae* BVI (formerly *Cafeteria roenbergensis* BVI), and predicted proteins from *Proteromonas lacertae* were used for comparative genomics analyses (Hackl et al. 2020; Záhonová et al. 2023). The genome assembly, transcripts, and proteins for *C. burkhardae* were downloaded from GenBank under accession GCA\_008330645.1. The genome sequence for *Proteromonas lacertae* was downloaded from GenBank under accession GCA\_002245135.1. As no predicted proteins or RNA-seq data were available for *P. lacertae*, genes were predicted from this genome using the BRAKER3 pipeline, using OrthoDB11 Eukaryota protein sequences as evidence. Proteins from all *Blastocystis* assemblies, *C. burkhardae*, and *P. lacertae* were annotated using a combination of InterProScan version 5.66 (Jones et al. 2014), DeepLoc2 to predict protein localization (Thumuluri et al. 2022), and dbCAN version 4.0.0 to annotate carbohydrate-active enzymes (Zhang et al. 2018). Orthologous sequences were determined using OrthoFinder2 with diamond as the search algorithm and mcl as the clustering algorithm (Li et al. 2003; Buchfink et al. 2015; Emms and Kelly 2019).

Genes related to cilia and flagella, microtubule motor proteins, signal transduction, ion channels, and nucleotide cyclase were identified using either GO categories or Interpro domains corresponding to these categories and are listed in Supplemental Table S4. Carbohydrate-degrading enzymes were identified based on the gene annotation methods mentioned above; specifically, polygalacturonase enzymes were identified with the PANTHER domain PTHR33928, beta-D-xylosidase with the Interpro domain IPR044993, a-L-arabinofuranosidase with the Interpro domain IPR010720, a-L-rhamnosidase with the PANTHER domain PTHR34987, and the GH154 arabinogalactanase with the PANTHER domain PTHR35339.

### Identifying motifs adjacent to transcript ends

To identify motifs enriched downstream from transcript ends, we extracted a 60-bp window upstream of and downstream from all annotated transcript ends in all *Blastocystis* genomes sequenced here, as well as *P. lacertae* and *C. burkhardae*. Motifs were identified separately in each genome using STREME version 5.5.7 (Bailey 2021). A motif similar to the one identified by Klimeš et al. (2014) was identified in both ST1, both ST3, and the ST4 human isolate, but no significant and informative motifs were identified in the tortoise-isolated *Blastocystis* isolates or in the *P. lacertae* or *C. burkhardae* genomes. We then combined the sequences from

all human isolates and ran STREME on this combined data set to generate a sequence motif (Fig. 2).

To determine enrichment of this motif in all genomes, we searched all transcript ends for matches to a degenerate version of the core region of the sequence motif, TGTTGTT, allowing up to two mismatches. As this motif is inherently an AT-rich sequence, the probability of observing it by chance is a function of the GC content of the sequence that is searched. We calculated the expected probability of seeing the 7-bp motif in each genome given the transcript window GC content and the number of transcripts, and calculated the enrichment of this motif as the log of the observed motif counts divided by the background expectation value (Fig. 2).

### Strain and species phylogenies

The *Blastocystis* genus phylogeny was constructed using 18S rRNA sequences deposited in GenBank (Supplemental Table S1), along with 18S rRNA sequences extracted from each *Blastocystis* assembly and from the *Proteromonas lacertae* genome as an outgroup. Sequences were aligned with MAFFT v7.505 (Katoh and Standley 2013) and a maximum likelihood phylogeny constructed using IQ-TREE version 2.3.5 (Minh et al. 2020) using with the GTR sequence model, 1000 ultrafast bootstrap and SH-aLRT replicates, and rooted on *P. lacertae*.

To construct a species phylogeny of all species and strains with genomic data used in this study, 13 conserved protein-coding genes identified with BUSCO version 5.6.1 as described above were extracted from *Cafeteria burkhardae*, *Proteromonas lacertae*, and all *Blastocystis* strains sequenced here. Proteins were aligned individually with MAFFT v7.505 and concatenated. Best-fit models for each partition were selected using a relaxed hierarchical clustering algorithm as implemented by ModelFinder in IQ-TREE version 2.3.5 (Chernomor et al. 2016; Kalyaanamoorthy et al. 2017; Minh et al. 2020); 1000 ultrafast bootstrap and SH-aLRT replicates were performed.

### Gene contamination and horizontal gene transfer screens

*Blastocystis* genomes were screened for bacterial contamination and for possible horizontal gene transfer events using a modified version of an alien index score (Gladyshev et al. 2008; Wisecaver et al. 2016). The alien index score compares the best bit score of a query sequence to a group of related taxa versus to all other unrelated groups and normalizes this score by the maximum possible bit score of the query sequence. It is determined by the formula  $AI = \frac{bbsO}{bbsS} - \frac{bbsI}{bbsS}$ , where *bbsO* is the bit score of the best hit to a species outside of the group lineage, *bbsI* is the bit score of the best hit to a species within the group lineage (skipping self hits), and *bbsS* is the bit score of the query aligned to itself. The alien index was calculated for each *Blastocystis* protein by querying proteins against the NCBI NR database using DIAMOND version 2.1.6 (Buchfink et al. 2015) (see Data access). The self-group was designated as *Blastocystis* (taxid: 12967), and the group lineage was set as all eukaryotes (taxid: 2759).

As an additional control for whether our genomes had high levels of genome contamination, we determined what fraction of genes with high alien index scores were likely transcribed by *Blastocystis*. Our RNA-seq strategy involved poly(A) purification, which removes non-polyadenylated transcripts. As polyadenylation is unique to eukaryotes, this removes bacterial transcripts. We quantified gene expression using kallisto version v0.48.0 (Bray et al. 2016) and determined whether genes with alien index scores greater than 0.2 were expressed and therefore likely truly integrated into the *Blastocystis* genomes. The number of genes with

alien index scores above 0.2 ranged from 59 to 81 genes across all sequenced genomes, and >85% were expressed in all genomes. For identifying novel cases of HGT, genes with alien index scores >0.2 that were expressed at TPM > 1 and had orthologs in one or more other *Blastocystis* genomes were further examined for evidence of horizontal gene transfer with gene tree reconstruction. Requiring alien index scores >0.2 enhances the confidence that the identified genes originated in other lineages, although we acknowledge that this is a conservative cutoff and the increased confidence may come at the expense of potentially missing some cases of HGT. We did not use this cutoff for analysis of previously identified genes of HGT and instead performed phylogenetic reconstruction of all previously identified genes (Eme et al. 2017).

### Gene tree reconstruction for horizontal transfer

Phylogenetic trees for putative horizontal gene transfer candidates were constructed from all diamond BLASTP hits using the NCBI NR database clustered at 90% sequence identity and 90% sequence length (Buchfink et al. 2015). Sequence hits that were outliers in length were excluded from downstream analyses. Protein sequences were aligned with MAFFT v7.505 (Katoh and Standley 2013), and maximum likelihood phylogenies were constructed using IQ-TREE version 2.3.5 using ModelFinder to determine the best-fit substitution model, and with 1000 ultrafast bootstrap replicates and 1000 replicates of the SH-like approximate likelihood ratio test (Guindon et al. 2010). Branches with SH-aLRT support less than 70 and UF-boot less than 80 were collapsed and trees were midpoint rooted before being examined for horizontal transfer.

### Data access

The genome assemblies and gene annotations generated in this study have been submitted to the NCBI BioProject database (<https://www.ncbi.nlm.nih.gov/bioproject/>) under accession numbers PRJNA1084774, PRJNA1185195, PRJNA1185180, PRJNA1084796, PRJNA1084798, PRJNA1084795, PRJNA1084799, and PRJNA1084775, and are also available as Supplemental Material. The RNA sequencing generated for *Blastocystis* strains has been submitted to the NCBI BioProject database under accession number PRJNA1041441. All alignments and phylogenies generated in this work, along with gene annotations for the *Proteromonas lacertae* gene annotations, are available as Supplemental Material and at Figshare ([https://figshare.com/projects/Blastocystis\\_genomes/186136](https://figshare.com/projects/Blastocystis_genomes/186136)). Code required to calculate the alien index is available at GitHub (<https://github.com/allind/alienindex>) and as Supplemental Code 1. All other code required to reproduce this work is available at GitHub (<https://github.com/allind/blastannotate>) and also as Supplemental Code 2.

### Competing interest statement

The authors declare no competing interests.

### Acknowledgments

We thank members of the Pollard lab and the Bhatt lab for helpful discussions. We thank Maggie Brown and Southern Grace Reptiles for providing samples for *Blastocystis* isolation from tortoises. This work was supported by National Heart, Lung, and Blood Institute (NHLBI) grant #R01-HL160862, Chan Zuckberg Biohub SF, and Gladstone Institutes to K.S.P, by the Benioff Center for Microbiome Medicine Trainee Pilot Award, National Institute of Allergy and Infectious Diseases (NIAID) award K22AI173181-02, and Georgia Institute of Technology to A.L.L. A.S.B. is supported

by National Institutes of Health grants R01AI143757 and R01AI148623, as well as a Stand Up 2 Cancer grant and a Paul Allen Distinguished Investigator Award.

**Author contributions:** Conceptualization: A.L.L., A.S.B., and K.S.P.; methodology: A.L.L., N.A.M., E.R.G., A.S.B., and K.S.P.; investigation: A.L.L. and K.S.P.; resources: A.S.B. and K.S.P.; writing (original draft): A.L.L., N.A.M., E.R.G., A.S.B., and K.S.P.; writing (review and editing): A.L.L., N.A.M., E.R.G., A.S.B., and K.S.P.; visualization: A.L.L.; supervision: K.S.P. and A.S.B.; funding acquisition: A.L.L., K.S.P., and A.S.B.

## References

- Alfellani MA, Taner-Mulla D, Jacob AS, Imeede CA, Yoshikawa H, Stensvold CR, Clark CG. 2013. Genetic diversity of *Blastocystis* in livestock and zoo animals. *Protist* **164**: 497–509. doi:10.1016/j.protis.2013.05.003
- Asnicar F, Berry SE, Valdes AM, Nguyen LH, Piccinno G, Drew DA, Leeming E, Gibson R, Le Roy C, Khatib HA, et al. 2021. Microbiome connections with host metabolism and habitual diet from 1,098 deeply phenotyped individuals. *Nat Med* **27**: 321–332. doi:10.1038/s41591-020-01183-8
- Bailey TL. 2021. STREME: accurate and versatile sequence motif discovery. *Bioinformatics* **37**: 2834–2840. doi:10.1093/bioinformatics/btab203
- Beghini F, Pasolli E, Truong TD, Putignano L, Cacciò SM, Segata N. 2017. Large-scale comparative metagenomics of *Blastocystis*, a common member of the human gut microbiome. *ISME J* **11**: 2848–2863. doi:10.1038/ismej.2017.139
- Boreham PFL, Stenzel DJ. 1993. *Blastocystis* in humans and animals: morphology, biology, and epizootiology. In *Advances in parasitology* (ed. Baker JR, Muller R), Vol. 32, pp. 1–70. Academic Press, San Diego.
- Bray NL, Pimentel H, Melsted P, Pachter L. 2016. Near-optimal probabilistic RNA-seq quantification. *Nat Biotechnol* **34**: 525–527. doi:10.1038/nbt.3519
- Buchfink B, Xie C, Huson DH. 2015. Fast and sensitive protein alignment using DIAMOND. *Nat Methods* **12**: 59–60. doi:10.1038/nmeth.3176
- Cartmell A, Muñoz-Muñoz J, Briggs JA, Ndeh DA, Lowe EC, Baslé A, Terrapon N, Stott K, Heunis T, Gray J, et al. 2018. A surface endogalactanase in *Bacteroides thetaiotaomicron* confers keystone status for arabinogalactan degradation. *Nat Microbiol* **3**: 1314–1326. doi:10.1038/s41564-018-0258-8
- Chernomor O, von Haeseler A, Minh BQ. 2016. Terrace aware data structure for phylogenomic inference from supermatrices. *Syst Biol* **65**: 997–1008. doi:10.1093/sysbio/syw037
- David LA, Maurice CF, Carmody RN, Gootenberg DB, Button JE, Wolfe BE, Ling AV, Devlin AS, Vanara Y, Fischbach MA, et al. 2014. Diet rapidly and reproducibly alters the human gut microbiome. *Nature* **505**: 559–563. doi:10.1038/nature12820
- del Campo J, Bass D, Keeling PJ. 2020. The eukaryome: diversity and role of microeukaryotic organisms associated with animal hosts. *Funct Ecol* **34**: 2045–2054. doi:10.1111/1365-2435.13490
- De Lorenzo G, Ferrari S. 2002. Polygalacturonase-inhibiting proteins in defense against phytopathogenic fungi. *Curr Opin Plant Biol* **5**: 295–299. doi:10.1016/S1369-5266(02)00271-6
- Deng Q, Sun X, Gao D, Wang Y, Liu Y, Li N, Wang Z, Liu M, Wang J, Wang Q. 2023. Characterization of two novel rumen-derived exo-polygalacturonases: catalysis and molecular simulations. *Microorganisms* **11**: 760. doi:10.3390/microorganisms11030760
- Denoeud F, Roussel M, Noel B, Wawrzyniak I, Da Silva C, Diogon M, Viscogliosi E, Brochier-Armanet C, Couloux A, Poulain J, et al. 2011. Genome sequence of the stramenopile *Blastocystis*, a human anaerobic parasite. *Genome Biol* **12**: R29. doi:10.1186/gb-2011-12-3-r29
- Dobin A, Davis CA, Schlesinger F, Drenkow J, Zaleski C, Jha S, Batut P, Chaisson M, Gingeras TR. 2013. STAR: ultrafast universal RNA-seq aligner. *Bioinformatics* **29**: 15–21. doi:10.1093/bioinformatics/bts635
- Eme L, Gentekaki E, Curtis B, Archibald JM, Roger AJ. 2017. Lateral gene transfer in the adaptation of the anaerobic parasite *Blastocystis* to the gut. *Curr Biol CB* **27**: 807–820. doi:10.1016/j.cub.2017.02.003
- Emms DM, Kelly S. 2019. OrthoFinder: phylogenetic orthology inference for comparative genomics. *Genome Biol* **20**: 238. doi:10.1186/s13059-019-1832-y
- Flynn JM, Hubble R, Goubert C, Rosen J, Clark AG, Feschotte C, Smit AF. 2020. RepeatModeler2 for automated genomic discovery of transposable element families. *Proc Natl Acad Sci* **117**: 9451–9457. doi:10.1073/pnas.1921046117
- Gabriel L, Bruna T, Hoff KJ, Ebel M, Lomsadze A, Borodovsky M, Stanke M. 2024. BRAKER3: fully automated genome annotation using RNA-seq and protein evidence with GeneMark-ETP, AUGUSTUS, and TSEBRA. *Genome Res* **34**: 769–777. doi:10.1101/gr.278090.123
- Gantois N, Lamot A, Seesao Y, Creusy C, Li L-L, Monchy S, Benamrouz-Vanneste S, Karpouzopoulos J, Bourgain J-L, Rault C, et al. 2020. First report on the prevalence and subtype distribution of *Blastocystis* sp. in edible marine fish and marine mammals: a large scale-study conducted in Atlantic northeast and on the coasts of northern France. *Microorganisms* **8**: 460. doi:10.3390/microorganisms8030460
- Gentekaki E, Curtis BA, Stairs CW, Klimeš V, Eliáš M, Salas-Leiva DE, Herman EK, Eme L, Arias MC, Henrissat B, et al. 2017. Extreme genome diversity in the hyper-prevalent parasitic eukaryote *Blastocystis*. *PLoS Biol* **15**: e2003769. doi:10.1371/journal.pbio.2003769
- Gladyshev EA, Meselson M, Arkhipova IR. 2008. Massive horizontal gene transfer in bdelloid rotifers. *Science* **320**: 1210–1213. doi:10.1126/science.1156407
- Godoy-Vitorino F, Goldfarb KC, Karaoz U, Leal S, Garcia-Amado MA, Hugenholtz P, Tringe SG, Brodie EL, Dominguez-Bello MG. 2012. Comparative analyses of foregut and hindgut bacterial communities in hoatzins and cows. *ISME J* **6**: 531–541. doi:10.1038/ismej.2011.131
- Gough R, Barratt J, Stark D, Ellis J. 2020. Diversity profiling of xenic cultures of *Dientamoeba fragilis* following systematic antibiotic treatment and prospects for genome sequencing. *Parasitology* **147**: 29–38. doi:10.1017/S0031182019001173
- Guillot L, Kim H, Traore Y, Moreau P, Lafite P, Coquoin V, Nuccio S, de Vaumas R, Daniellou R. 2019. Biochemical characterization of the  $\alpha$ -L-rhamnosidase DTrha from *Dictyoglomus thermophilum*: application to the selective derhamnosylation of natural flavonoids. *ACS Omega* **4**: 1916–1922. doi:10.1021/acsomega.8b03186
- Guindon S, Dufayard J-F, Lefort V, Anisimova M, Hordijk W, Gascuel O. 2010. New algorithms and methods to estimate maximum-likelihood phylogenies: assessing the performance of PhyML 3.0. *Syst Biol* **59**: 307–321. doi:10.1093/sysbio/syq010
- Hackl T, Martin R, Barenhoff K, Duponchel S, Heider D, Fischer MG. 2020. Four high-quality draft genome assemblies of the marine heterotrophic nanoflagellate *Cafeteria roenbergensis*. *Sci Data* **7**: 29. doi:10.1038/s41597-020-0363-4
- Hoang DT, Chernomor O, von Haeseler A, Minh BQ, Vinh LS. 2018. UFBoot2: improving the ultrafast bootstrap approximation. *Mol Biol Evol* **35**: 518–522. doi:10.1093/molbev/msx281
- Jinatham V, Maxamhud S, Pobluechai S, Tsaousis AD, Gentekaki E. 2021. *Blastocystis* one health approach in a rural community of northern Thailand: prevalence, subtypes and novel transmission routes. *Front Microbiol* **12**: 746340. doi:10.3389/fmicb.2021.746340
- Johnson J-LF, Leroux MR. 2010. cAMP and cGMP signaling: sensory systems with prokaryotic roots adopted by eukaryotic cilia. *Trends Cell Biol* **20**: 435–444. doi:10.1016/j.tcb.2010.05.005
- Jones P, Binns D, Chang H-Y, Fraser M, Li W, McAnulla C, McWilliam H, Maslen J, Mitchell A, Nuka G, et al. 2014. Interproscan 5: genome-scale protein function classification. *Bioinformatics* **30**: 1236–1240. doi:10.1093/bioinformatics/btu031
- Kalyaanamoorthy S, Minh BQ, Wong TKF, von Haeseler A, Jermin LS. 2017. ModelFinder: fast model selection for accurate phylogenetic estimates. *Nat Methods* **14**: 587–589. doi:10.1038/nmeth.4285
- Kang DD, Li F, Kirton E, Thomas A, Egan R, An H, Wang Z. 2019. MetaBAT 2: an adaptive binning algorithm for robust and efficient genome reconstruction from metagenome assemblies. *PeerJ* **7**: e7359. doi:10.7717/peerj.7359
- Katoh K, Standley DM. 2013. MAFFT multiple sequence alignment software version 7: improvements in performance and usability. *Mol Biol Evol* **30**: 772–780. doi:10.1093/molbev/mst010
- Keeling PJ, Burki F, Wilcox HM, Allam B, Allen EE, Amaral-Zettler LA, Armbrust EV, Archibald JM, Bharti AK, Bell CJ, et al. 2014. The Marine Microbial Eukaryote Transcriptome Sequencing Project (MMETSP): illuminating the functional diversity of eukaryotic life in the oceans through transcriptome sequencing. *PLoS Biol* **12**: e1001889. doi:10.1371/journal.pbio.1001889
- Khaled S, Gantois N, Ly AT, Senghor S, Even G, Dautel E, Dejager R, Sawant M, Baydoun M, Benamrouz-Vanneste S, et al. 2020. Prevalence and subtype distribution of *Blastocystis* sp. in Senegalese school children. *Microorganisms* **8**: 1408. doi:10.3390/microorganisms8091408
- Klimeš V, Gentekaki E, Roger AJ, Eliáš M. 2014. A large number of nuclear genes in the human parasite *Blastocystis* require mRNA polyadenylation to create functional termination codons. *Genome Biol Evol* **6**: 1956–1961. doi:10.1093/gbe/evu146
- Kolmogorov M, Yuan J, Lin Y, Pevzner PA. 2019. Assembly of long, error-prone reads using repeat graphs. *Nat Biotechnol* **37**: 540–546. doi:10.1038/s41587-019-0072-8
- Kolmogorov M, Bickhart DM, Behsaz B, Gurevich A, Rayko M, Shin SB, Kuhn K, Yuan J, Polevikov E, Smith TPL, et al. 2020. metaFlye: scalable long-read metagenome assembly using repeat graphs. *Nat Methods* **17**: 1103–1110. doi:10.1038/s41592-020-00971-x

- Kostka M. 2017. Opalinata. In *Handbook of the Protists* (ed. Archibald JM, et al.), pp. 543–565. Springer International Publishing, Cham, Switzerland.
- Kuznetsov D, Tegenfeldt F, Manni M, Seppey M, Berkeley M, Kriventseva EV, Zdobnov EM. 2022. OrthoDB v11: annotation of orthologs in the widest sampling of organismal diversity. *Nucleic Acids Res* **51**: D445–D451. doi:10.1093/nar/gkac998
- Lagaert S, Pollet A, Courtin CM, Volckaert G. 2014.  $\beta$ -Xylosidases and  $\alpha$ -L-arabinofuranosidases: accessory enzymes for arabinoxylan degradation. *Biotechnol Adv* **32**: 316–332. doi:10.1016/j.biotechadv.2013.11.005
- Leckenby A, Hall N. 2015. Genomic changes during evolution of animal parasitism in eukaryotes. *Curr Opin Genet Dev* **35**: 86–92. doi:10.1016/j.gde.2015.11.001
- Levy Karin E, Mirdita M, Söding J. 2020. Metaeuk—sensitive, high-throughput gene discovery, and annotation for large-scale eukaryotic metagenomics. *Microbiome* **8**: 48. doi:10.1186/s40168-020-00808-x
- Li H. 2018. Minimap2: pairwise alignment for nucleotide sequences. *Bioinformatics* **34**: 3094–3100. doi:10.1093/bioinformatics/bty191
- Li L, Stoeckert CJ, Roos DS. 2003. OrthoMCL: identification of ortholog groups for eukaryotic genomes. *Genome Res* **13**: 2178–2189. doi:10.1101/gr.1224503
- Maloney JG, Santin M. 2021. Mind the gap: new full-length sequences of *Blastocystis* subtypes generated via Oxford nanopore minION sequencing allow for comparisons between full-length and partial sequences of the small subunit of the ribosomal RNA gene. *Microorganisms* **9**: 997. doi:10.3390/microorganisms9050997
- Manni M, Berkeley MR, Seppey M, Simão FA, Zdobnov EM. 2021. BUSCO update: novel and streamlined workflows along with broader and deeper phylogenetic coverage for scoring of eukaryotic, prokaryotic, and viral genomes. *Mol Biol Evol* **38**: 4647–4654. doi:10.1093/molbev/msab199
- McCutcheon JP, Moran NA. 2012. Extreme genome reduction in symbiotic bacteria. *Nat Rev Microbiol* **10**: 13–26. doi:10.1038/nrmicro2670
- McLay T. 2017. High quality DNA extraction protocol from recalcitrant plant tissues v1. <https://www.protocols.io/view/high-quality-dna-extraction-protocol-from-recalcit-i8jchun> (Accessed January 3, 2025). protocols.io doi:10.17504/protocols.io.i8jchun
- Minh BQ, Schmidt HA, Chernomor O, Schrempf D, Woodhams MD, von Haeseler A, Lanfear R. 2020. IQ-TREE 2: new models and efficient methods for phylogenetic inference in the genomic era. *Mol Biol Evol* **37**: 1530–1534. doi:10.1093/molbev/msaa015
- Moeller AH, Caro-Quintero A, Mjungu D, Georgiev AV, Lonsdorf EV, Muller MN, Pusey AE, Peeters M, Hahn BH, Ochman H. 2016. Cospeciation of gut microbiota with hominids. *Science* **353**: 380–382. doi:10.1126/science.aaf3951
- Moss EL, Maghini DG, Bhatt AS. 2020. Complete, closed bacterial genomes from microbiomes using nanopore sequencing. *Nat Biotechnol* **38**: 701–707. doi:10.1038/s41587-020-0422-6
- Nash AK, Auchtung TA, Wong MC, Smith DP, Gesell JR, Ross MC, Stewart CJ, Metcalf GA, Muzny DM, Gibbs RA, et al. 2017. The gut mycobiome of the Human Microbiome Project healthy cohort. *Microbiome* **5**: 153. doi:10.1186/s40168-017-0373-4
- Nieves-Ramírez ME, Partida-Rodríguez O, Laforest-Lapointe I, Reynolds LA, Brown EM, Valdez-Salazar A, Morán-Silva P, Rojas-Velázquez L, Morien E, Parfrey LW, et al. 2018. Asymptomatic intestinal colonization with protist *Blastocystis* is strongly associated with distinct microbiome ecological patterns. *mSystems* **3**: e00007-18. doi:10.1128/mSystems.00007-18
- Pertea M, Pertea GM, Antonescu CM, Chang T-C, Mendell JT, Salzberg SL. 2015. StringTie enables improved reconstruction of a transcriptome from RNA-seq reads. *Nat Biotechnol* **33**: 290–295. doi:10.1038/nbt.3122
- Piperni E, Nguyen LH, Manghi P, Kim H, Pasolli E, Andreu-Sánchez S, Arrè A, Birmingham KM, Blanco-Míguez A, Manara S, et al. 2024. Intestinal *Blastocystis* is linked to healthier diets and more favorable cardiometabolic outcomes in 56,989 individuals from 32 countries. *Cell* **187**: 4554–4570.e18. doi:10.1016/j.cell.2024.06.018
- Ranallo-Benavidez TR, Jaron KS, Schatz MC. 2020. GenomeScope 2.0 and Smudgeplot for reference-free profiling of polyploid genomes. *Nat Commun* **11**: 1432. doi:10.1038/s41467-020-14998-3
- Saary P, Mitchell AL, Finn RD. 2020. Estimating the quality of eukaryotic genomes recovered from metagenomic analysis with EukCC. *Genome Biol* **21**: 244. doi:10.1186/s13059-020-02155-4
- Santin M, Figueiredo A, Molokin A, George NS, Köster PC, Dashti A, González-Barrio D, Carmena D, Maloney JG. 2024. Division of *Blastocystis* ST10 into three new subtypes: ST42-ST44. *J Eukaryot Microbiol* **71**: e12998. doi:10.1111/jeu.12998
- Scanlan PD, Marchesi JR. 2008. Micro-eukaryotic diversity of the human distal gut microbiota: qualitative assessment using culture-dependent and -independent analysis of faeces. *ISME J* **2**: 1183–1193. doi:10.1038/ismej.2008.76
- Scanlan PD, Stensvold CR. 2013. *Blastocystis*: getting to grips with our guileful guest. *Trends Parasitol* **29**: 523–529. doi:10.1016/j.pt.2013.08.006
- Scanlan PD, Stensvold CR, Rajilić-Stojanović M, Heilig HGHJ, De Vos WM, O'Toole PW, Cotter PD. 2014. The microbial eukaryote *Blastocystis* is a prevalent and diverse member of the healthy human gut microbiota. *FEMS Microbiol Ecol* **90**: 326–330. doi:10.1111/1574-6941.12396
- Schultz DT, Haddock SHD, Bredeson JV, Green RE, Simakov O, Rokhsar DS. 2023. Ancient gene linkages support ctenophores as sister to other animals. *Nature* **618**: 110–117. doi:10.1038/s41586-023-05936-6
- Šimková H, Câmara AS, Mascher M. 2024. Hi-C techniques: from genome assemblies to transcription regulation. *J Exp Bot* **75**: 5357–5365. doi:10.1093/jxb/erae085
- Smit A, Hubley R, Green P. 2013. RepeatMasker Open-4.0. <http://www.repeatmasker.org> (Accessed January 10, 2015).
- Sommer F, Bäckhed F. 2013. The gut microbiota—masters of host development and physiology. *Nat Rev Microbiol* **11**: 227–238. doi:10.1038/nrmicro2974
- Stensvold CR, Clark CG. 2020. Pre-empting Pandora's box: *Blastocystis* subtypes revisited. *Trends Parasitol* **36**: 229–232. doi:10.1016/j.pt.2019.12.009
- Stensvold CR, Suresh GK, Tan KSW, Thompson RCA, Traub RJ, Viscogliosi E, Yoshikawa H, Clark CG. 2007. Terminology for *Blastocystis* subtypes – a consensus. *Trends Parasitol* **23**: 93–96. doi:10.1016/j.pt.2007.01.004
- Stevens CE, Hume ID. 1995. *Comparative physiology of the vertebrate digestive system*, 2nd ed. Cambridge University Press, Cambridge.
- Storer J, Hubley R, Rosen J, Wheeler TJ, Smit AF. 2021. The Dfam community resource of transposable element families, sequence models, and genome annotations. *Mob DNA* **12**: 2. doi:10.1186/s13100-020-00230-y
- Tan KSW. 2008. New insights on classification, identification, and clinical relevance of *Blastocystis* spp. *Clin Microbiol Rev* **21**: 639–665. doi:10.1128/CMR.00022-08
- Thorman AW, Adkins G, Conrey SC, Burrell AR, Yu Y, White B, Burke R, Haslam D, Payne DC, Staat MA, et al. 2023. Gut microbiome composition and metabolic capacity differ by FUT2 secretor status in exclusively breastfed infants. *Nutrients* **15**: 471. doi:10.3390/nu15020471
- Thumuluri V, Almagro Armenteros JJ, Johansen AR, Nielsen H, Winther O. 2022. DeepLoc 2.0: multi-label subcellular localization prediction using protein language models. *Nucleic Acids Res* **50**: W228–W234. doi:10.1093/nar/gkac278
- Vaser R, Sović I, Nagarajan N, Šikić M. 2017. Fast and accurate de novo genome assembly from long uncorrected reads. *Genome Res* **27**: 737–746. doi:10.1101/gr.214270.116
- Venturini L, Caim S, Kaithakottil GG, Mapleson DL, Swarbreck D. 2018. Leveraging multiple transcriptome assembly methods for improved gene structure annotation. *GigaScience* **7**: giy093. doi:10.1093/giga-science/gy093
- Wang SE, Amir AS, Nguyen T, Poole AM, Simoes-Barbosa A. 2018. Spliceosomal introns in *Trichomonas vaginalis* revisited. *Parasit Vectors* **11**: 607. doi:10.1186/s13071-018-3196-7
- West PT, Probst AJ, Grigoriev IV, Thomas BC, Banfield JF. 2018. Genome-reconstruction for eukaryotes from complex natural microbial communities. *Genome Res* **28**: 569–580. doi:10.1101/gr.228429.117
- Wick RR, Holt KE. 2022. Polypolish: short-read polishing of long-read bacterial genome assemblies. *PLoS Comput Biol* **18**: e1009802. doi:10.1371/journal.pcbi.1009802
- Wilihoelt U, Campos-Góngora E, Touzni S, Bruchhaus I, Tannich E. 2001. Introns of *Entamoeba histolytica* and *Entamoeba dispar*. *Protist* **152**: 149–156. doi:10.1078/1434-4610-00053
- Wisecaver JH, Alexander WG, King SB, Hittinger CT, Rokas A. 2016. Dynamic evolution of nitric oxide detoxifying flavohemoglobins, a family of single-protein metabolic modules in bacteria and eukaryotes. *Mol Biology Evol* **33**: 1979–1987. doi:10.1093/molbev/msw073
- Yadav M, Verma MK, Chauhan NS. 2018. A review of metabolic potential of human gut microbiome in human nutrition. *Arch Microbiol* **200**: 203–217. doi:10.1007/s00203-017-1459-x
- Yang JK, Yoon HJ, Ahn HJ, Lee BI, Pedelacq J-D, Liang EC, Berendzen J, Laivenieks M, Vieille C, Zeikus GJ, et al. 2004. Crystal structure of beta-D-xylosidase from *Thermoanaerobacterium saccharolyticum*, a family 39 glycoside hydrolase. *J Mol Biol* **335**: 155–165. doi:10.1016/j.jmb.2003.10.026
- Yoshikawa H, Koyama Y, Tsuchiya E, Takami K. 2016. *Blastocystis* phylogeny among various isolates from humans to insects. *Parasitol Int* **65**: 750–759. doi:10.1016/j.parint.2016.04.004
- Záhonová K, Low RS, Warren CJ, Cantoni D, Herman EK, Yiangou L, Ribeiro CA, Phanprasert Y, Brown IR, Rueckert S, et al. 2023. Evolutionary analysis of cellular reduction and anaerobicity in the hyper-prevalent gut microbe *Blastocystis*. *Curr Biol* **33**: 2449–2464.e8. doi:10.1016/j.cub.2023.05.025
- Zhang H, Yohe T, Huang L, Entwistle S, Wu P, Yang Z, Busk PK, Xu Y, Yin Y. 2018. dbCAN2: a meta server for automated carbohydrate-active

Lind et al.

---

- enzyme annotation. *Nucleic Acids Res* **46**: W95–W101. doi:10.1093/nar/gky418
- Zierdt CH. 1988. *Blastocystis hominis*, a long-misunderstood intestinal parasite. *Parasitol Today* **4**: 15–17. doi:10.1016/0169-4758(88)90049-X
- Zierdt CH, Williams RL. 1974. *Blastocystis hominis*: axenic cultivation. *Exp Parasitol* **36**: 233–243. doi:10.1016/0014-4894(74)90062-9
- Zimin AV, Marçais G, Puiu D, Roberts M, Salzberg SL, Yorke JA. 2013. The MaSuRCA genome assembler. *Bioinformatics* **29**: 2669–2677. doi:10.1093/bioinformatics/btt476

Received February 7, 2024; accepted in revised form April 10, 2025.